

Dynamical critical quantum sensing with a single parametrically-driven nonlinear resonator

Ken Chen,¹ Jia-Hao Lü,¹ Xin Zhu,¹ Hao-Long Zhang,¹ Wen Ning,¹ Zhen-Biao Yang,^{1,*} and Shi-Biao Zheng^{1,†}

¹*Fujian Key Laboratory of Quantum Information and Quantum Optics,
College of Physics and Information Engineering,
Fuzhou University, Fuzhou, Fujian 350108, China*

Critical phenomena of quantum systems are useful for enhancement of quantum sensing. We here investigate the performance of a sensing scheme, where the signal is encoded in the dynamically-evolving state of an oscillator, featuring a competition of the Kerr nonlinearity and parametric driving. We calculate the quantum Fisher information, and perform a simulation, which confirms the criticality-enabled enhancement. We further detail the response of one of the quadratures to the variation of the control parameter. The numerical results reveal that its inverted variance exhibits a diverging behavior at the critical point.

I. INTRODUCTION

The quantum phase transition (QPT) [1, 2] is an interdisciplinary subject across a variety of physical branches, ranging from condensed physics, statistical mechanics, and quantum optics. In addition to fundamental interest, critical phenomena near the QPT are a valuable resource for quantum technological applications, among which quantum metrology is a paradigmatic example [3–6]. Around the critical point of a QPT, the physical properties of a quantum system exhibit a ultra-sensitive response to variation of the control parameters, which enables the critical system to be used as a quantum sensor with an enhanced sensitivity. In recent years, many theoretical schemes have been proposed for criticality-enhanced quantum sensing in different systems, including the quantum Rabi model [7–9], the parametrically-driven Jaynes-Cummings model [10], and an Ising chain coupled to a cavity mode [11]. All these schemes are based on the capability to precisely control freedom degrees of a composite light-matter system near the critical point, which is a challenging task in experiment.

Recently, a novel scheme was proposed to realize critical quantum sensing with a single bosonic mode [12]. The quantum phase transition is driven by the combination of a Kerr nonlinearity and parametric driving [13]. This scenario is experimentally favorable as there is no need to control composite degrees of freedom. The parametric Kerr oscillator has been proposed to serve as a cat qubit for realizing fault-tolerant quantum computation [14, 15], and was demonstrated in a recent superconducting circuit experiment [16]. In Refs. [4, 17–26], the quantum sensor works in a steady state, whose dynamics was investigated in a dissipative-driven context. It remains an open question how much the criticality can benefit the performance of a quantum sensor based on the unitary dynamics of such a nonlinear resonator.

We here perform a detailed investigation on the dynamical critical quantum sensing with the parametrically-driven Kerr resonator. We characterize the performance of this quantum sensing by quantum Fisher information. The numerical results show that the Fisher information evolves in an oscillating pattern, with the height of the peak increases with the evolution times. In both the normal and superradiant phases, the local maxima of the Fisher information are dramatically increasing when the system is closer to the critical point. The simulated inverted variance of the squeezed quadrature of the resonator exhibits a diverging behavior at the critical point, evidencing the criticality-enhanced susceptibility.

II. THE PARAMETRICALLY-DRIVEN NONLINEAR RESONATOR

We start by considering the Kerr-resonator model, which has \mathbb{Z}_2 symmetry. The Hamiltonian can be written as ($\hbar = 1$)

$$H_{\text{Kerr}} = \omega \hat{a}^\dagger \hat{a} + \frac{\epsilon}{2} (\hat{a}^{\dagger 2} + \hat{a}^2) + \chi \hat{a}^{\dagger 2} \hat{a}^2. \quad (1)$$

where \hat{a} (\hat{a}^\dagger) is the annihilation (creation) operator for the resonator photon with the frequency ω , ϵ is the two-photon pump amplitude and χ is the strength of the Kerr nonlinearity.

First, we consider the case $\chi \rightarrow 0$ in the normal phase. Here we define $g = \epsilon/\omega$ and Eq. (1) can be rewritten in the following form as

$$H_{\text{np}} = \omega [\hat{a}^\dagger \hat{a} + \frac{g}{2} (\hat{a}^{\dagger 2} + \hat{a}^2)]. \quad (2)$$

Furthermore, Eq. (2) can be diagonalized exactly by introducing the bosonic squeezed operator $\hat{S}(r) = e^{\frac{r}{2}(\hat{a}^{\dagger 2} - \hat{a}^2)}$ where r is the squeezing parameter. The squeezing transformation leads to

$$H'_{\text{np}} = S^\dagger(r) H_{\text{Kerr}} S(r). \quad (3)$$

* zbyang@fzu.edu.cn

† t96034@fzu.edu.cn

When the coefficient of the $(a^{\dagger 2} + a^2)$ term vanishes, H_{Kerr} is diagonalized as $H'_{\text{np}} = e_{\text{np}} a^{\dagger} a + E_{\text{np}}$ with the excitation energy $e_{\text{np}} = \omega \sqrt{1 - g^2}$ and the ground-state energy $E_{\text{np}} = \frac{\omega}{2} \sqrt{1 - g^2} - \frac{\omega}{2}$. The squeezing parameter is given by

$$r_{\text{np}} = \frac{1}{4} \ln R_0 \quad (R_0 = \frac{1 - g}{1 + g}), \quad (4)$$

which diverges at the critical point. We remark that the excitation energy e_{np} is real only when $g \leq 1$. Meanwhile, $g < 1$ is a sufficient condition making r a significant number, i.e., the inequality $R_0 > 0$ is always satisfied. In the normal phase, the eigenstates and eigenenergies of H_{np} are

$$\begin{aligned} |\phi_{\text{np}}^n\rangle &= S(r)|n\rangle, \\ E_{\text{np}}^n &= n e_{\text{np}} + E_{\text{np}}. \end{aligned} \quad (5)$$

When $g > 1$, we see that the excitation energy e_{np} is imaginary, i.e., in the superradiant phase. In order to have a profound understanding of the superradiant phase, let us apply a displacement operator such that $D(\alpha) = e^{\alpha a^{\dagger} - \alpha^* a}$ in the original Hamiltonian H_{Kerr} , which corresponds to the transformation

$$D^{\dagger}(\alpha) a D(\alpha) = a + \alpha. \quad (6)$$

Therefore, the original Hamiltonian H_{Kerr} is transformed to

$$\begin{aligned} H_{\text{sp}} &= D^{\dagger}(\alpha) H_{\text{Kerr}} D(\alpha) \\ &= H_{\text{sp}}^{(1)} + H_{\text{sp}}^{(2)} + H_{\text{sp}}^{(3)} + \text{const}. \end{aligned} \quad (7)$$

where

$$\begin{aligned} H_{\text{sp}}^{(1)} &= (2\chi\alpha^2\alpha^* + \epsilon\alpha^* + \omega\alpha)a^{\dagger} + \text{H.c.}, \\ H_{\text{sp}}^{(2)} &= (4\chi|\alpha|^2 + \omega)a^{\dagger}a + (\chi\alpha^2 + \frac{\epsilon}{2})a^{\dagger 2} + (\chi\alpha^2 + \frac{\epsilon}{2})a^2, \\ H_{\text{sp}}^{(3)} &= \chi(a^{\dagger 2}a^2 + 2\alpha a^{\dagger 2}a + 2\alpha^* a^{\dagger}a^2), \\ \text{const} &= \chi|\alpha|^4 + \frac{\epsilon}{2}\alpha^{*2} + \frac{\epsilon}{2}\alpha^2 + \omega|\alpha|^2. \end{aligned} \quad (8)$$

The equilibrium points are defined by the linear equation which can be found by imposing $H_{\text{sp}}^{(1)} = 0$, i.e., $2\chi\alpha^2\alpha^* + \epsilon\alpha^* + \omega\alpha = 0$. Setting $\alpha = |\alpha|e^{i\theta}$, we find two solutions for $g > 1$:

$$\begin{aligned} |\alpha|^2 &= \omega \frac{g - 1}{2\chi}, \\ \theta &= \pm \frac{\pi}{2}. \end{aligned} \quad (9)$$

Substituting the solution into Eq. (7), the effective Hamiltonians in the superradiant phase can be obtained as follows

$$H_{\text{sp}\pm} = \omega(2g - 1)a^{\dagger}a + \frac{\omega}{2}(a^{\dagger 2} + a^2) + O(\sqrt{\chi}). \quad (10)$$

It is necessary to stress that the Hamiltonians $H_{\text{sp}\pm}$ are the same in the limit of $\chi \rightarrow 0$ and thus the two solutions are degenerate. Since $\omega \sim \epsilon$ for $g \rightarrow 1$, the pump power and the pump-resonator detuning have an inseparable relationship, both increasing and decreasing at the same time. This means that increasing the pump gives rise to the displacement of the new equilibrium points of the state.

Let us use the transformation $\tilde{H}_{\text{sp}\pm} = S^{\dagger}(r)H_{\text{sp}\pm}S(r)$ with the squeezing operator $S(r) = e^{\frac{r}{2}(a^{\dagger 2} - a^2)}$ where r is the squeezing parameter. Requiring that the coefficient of the $(a^{\dagger 2} + a^2)$ term vanishes, $\tilde{H}_{\text{sp}\pm}$ can be rewritten as

$$\tilde{H}_{\text{sp}\pm} = e_{\text{sp}} a^{\dagger} a + E_{\text{sp}}, \quad (11)$$

where the excitation energy $e_{\text{sp}} = 2\omega\sqrt{g(g-1)}$ is real only when $g > 1$ and the ground-state energy $E_{\text{sp}} = \omega\sqrt{g(g-1)} - \omega g + \frac{\omega}{2}$. Since $\alpha = \pm\alpha_s$ are two independent choices, $\tilde{H}_{\text{sp}\pm}$ have the same energy spectrum in the superradiant phase. In the superradiant phase, the eigenstates and eigenenergies of $\tilde{H}_{\text{sp}\pm}$ can be written as

$$\begin{aligned} |\phi_{\text{sp}}^n\rangle &= D(\pm\alpha_s)S(r_{\text{sp}})|n\rangle, \\ E_{\text{sp}}^n &= n e_{\text{sp}} + E_{\text{sp}}, \end{aligned} \quad (12)$$

where the squeezing parameter r_{sp} is

$$r_{\text{sp}} = \frac{1}{4} \ln \frac{g - 1}{g}. \quad (13)$$

From the above analytical derivations for the normal- and superradiant-phase Hamiltonians, one can easily see that the QPT in the system occurs at the phase boundary $g = 1$.

In Fig. 1(a), we can see that while the ground state energy $E(g)$ is continuous, $dE(g)/dg$ is discontinuous at $g = 1$, revealing the first-order nature of the QPT. In fact, one can quickly compute $E(g = 1) = -\omega/2$ according to E_{np} and E_{sp} . And as shown in Fig. 1(b), as g approaches 1, both excitation energies e_{np} and e_{sp} vanish at the phase boundary, which once again confirms that the appearance of the QPT.

Here we recall the Hamiltonian H'_{np} in the normal phase which provides a truthful description of the system ground state of the KRM. Although it is stable for $g < 1$, for $g \rightarrow 1$ the system undergoes a phase transition towards the superradiant phase.

The precise estimation of A (with $A = \epsilon$) obtained by performing measurements on the ground state of the system is a very important job. This precision is bounded by the quantum CR bound. Since the system is in a pure state, the formula of the QFI may be given by $\mathcal{I}_A = 4[|\langle \partial_A \phi_{\text{np}} | \partial_A \phi_{\text{np}} \rangle + (\langle \partial_A \phi_{\text{np}} | \phi_{\text{np}} \rangle)^2]$ [7]. In proximity of the QPT, the term which makes the dominant contribution is

$$\mathcal{I}_{A_{\text{np}}} \sim \frac{1}{2A^2(1 - g)^2} \quad (14)$$

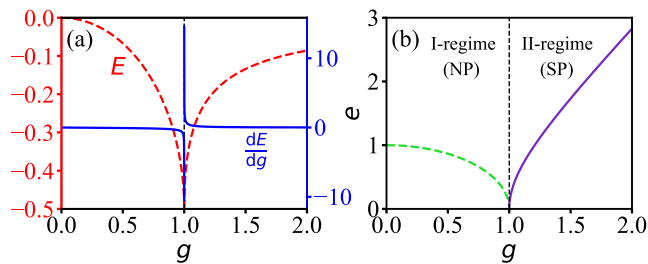


FIG. 1. Exact solutions of the Kerr-resonator model as a function of the parameter g for (a) the ground state energy E (red dashed line) and dE/dg (blue solid line) and (b) the excitation energy e in the normal phase (green dashed line) and in the superradiant phase (purple solid line).

which means that we can get the signal-to-noise ratio $\mathcal{Q}_{A_{\text{np}}} = A^2 \mathcal{I}_{A_{\text{np}}}$ from the estimation of ϵ .

In the superradiant phase, the ground-state of this Hamiltonian is a displaced squeezed state with displacing parameter $\alpha_s = i\sqrt{\frac{\omega(g-1)}{2\chi}}$ and squeezing parameter $r_{\text{sp}} = \frac{1}{4} \ln \frac{g-1}{g}$. Thus, we arrive at the two following states: $|\phi_{\text{sp}}^{\pm}\rangle = D(\pm\alpha_s)S(r_{\text{sp}})|0\rangle$. For both $|\phi_{\text{sp}}^+\rangle$ and $|\phi_{\text{sp}}^-\rangle$, we can compute directly the QFI.

According to the formula $\mathcal{I}_A = 4[\langle \partial_A \phi_{\text{sp}} | \partial_A \phi_{\text{sp}} \rangle + \langle (\partial_A \phi_{\text{sp}} | \phi_{\text{sp}}) \rangle^2]$, we can calculate directly the QFI as follows

$$\mathcal{I}_{A_{\text{sp}}} \sim \frac{g^2}{8A^2(g-1)^2} + \frac{\omega g^2}{2A^2\chi} \sqrt{\frac{\omega}{\epsilon(g-1)}}. \quad (15)$$

Notice that the second term becomes negligible when g goes to 1. Therefore, we can obtain $\mathcal{I}_{A_{\text{sp}}} \sim \frac{g^2}{8A^2(g-1)^2}$ in the superradiant phase.

As shown in Fig. (2), one can easily see that \mathcal{Q}_A diverges at the critical point $g = 1$ in the normal phase and in the superradiant phase. And thus we generally obtain an arbitrarily large estimation precision. This is in accordance with relevant studies on critical metrology in light-matter systems.

III. QUANTUM FISHER INFORMATION NEAR THE CRITICAL POINT

To further investigate quantum sensing based on the KRM, we apply a dynamic framework [8] which does not rely on particular initial states of the bosonic field mode or adiabatic evolution. In this framework, the QFI with respect to the parameter λ can be specified as $I_\lambda = 4\text{Var}[h_\lambda]_{|\psi\rangle}$, where $\text{Var}[h_\lambda]$ represents the variance of h_λ related to the initial state $|\psi\rangle$ and $h_\lambda = -i(\partial_\lambda U_\lambda^\dagger)U_\lambda = iU_\lambda^\dagger \partial_\lambda U_\lambda$ is the transformed local generator [27]. We choose the Hamiltonian $\hat{H}_\lambda = \hat{H}_0 + \lambda \hat{H}_1$, which satisfies the following equation [28]

$$[\hat{H}_\lambda, \hat{\zeta}] = \sqrt{\Delta} \hat{\zeta}, \quad (16)$$

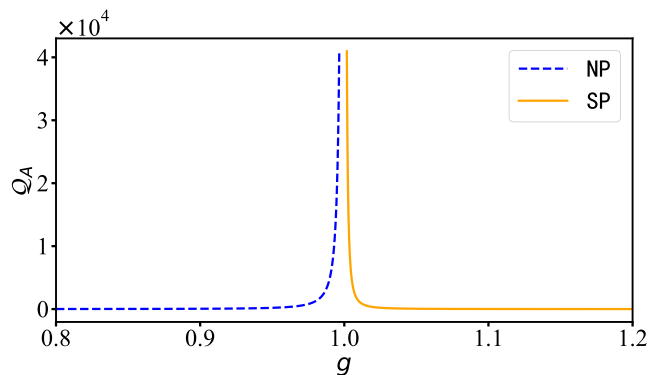


FIG. 2. Signal-to-noise ratio \mathcal{Q}_A versus g for the estimation of ϵ in the normal phase (blue dashed line) and in the superradiant phase (orange solid line).

where $\hat{\zeta} = i\sqrt{\Delta} \hat{P} - \hat{Q}$ with $\hat{P} = -i[\hat{H}_0, \hat{H}_1]$, $\hat{Q} = -[\hat{H}_\lambda, [\hat{H}_0, \hat{H}_1]]$ and Δ is relied on the parameter λ . The above \hat{H}_λ has an evenly spaced energy spectrum with the energy gap $\epsilon \sim \sqrt{\Delta}$ when $\Delta > 0$ and $\sqrt{\Delta}$ becomes imaginary if $\Delta < 0$ [8]. The QPT emerges when λ is equal to the critical point λ_c defined by $\Delta = 0$. Furthermore, the transformed local generator can be written in the following form as

$$h_\lambda = \hat{H}_1 t + \frac{\cos(\sqrt{\Delta}t) - 1}{\Delta} \hat{P} - \frac{\sin(\sqrt{\Delta}t) - \sqrt{\Delta}t}{\Delta \sqrt{\Delta}} \hat{Q}. \quad (17)$$

We remark that h_λ exhibits a divergent signature as $\Delta \rightarrow 0$ if $\sqrt{\Delta}t \simeq \mathcal{O}(1)$. According to Eq. (17), we can obtain the QFI as follows:

$$I_\lambda(t) \simeq 4 \frac{[\sin(\sqrt{\Delta}t) - \sqrt{\Delta}t]^2}{\Delta^3} \text{Var}[\hat{Q}]_{|\phi\rangle}. \quad (18)$$

Assuming $\sqrt{\Delta}t \simeq \mathcal{O}(1)$, the QFI scales with Δ as $I_\lambda \sim \Delta^{-3}$, which holds for general initial states $|\phi\rangle$ on condition that $\text{Var}[\hat{Q}]_{|\phi\rangle} \simeq \mathcal{O}(1)$ or even more general mixed states [8].

The Hamiltonian H_{np} satisfies the relation in Eq. (16), and we can obtain $\Delta_{\text{np}} = \omega^2 \Delta_{g_{\text{np}}}$ with $\Delta_{g_{\text{np}}} = 4(1-g^2)$. If $\Delta_{\text{np}} = 0$, i.e., $g = 1$, the phase transition happens. Applying a similar analysis by which we derive Eq. (18), the QFI with respect to the parameter g can be given as

$$\mathcal{I}_{g_{\text{np}}}(t) \simeq 16(1+g)^2 \frac{[\sin(\sqrt{\Delta_{g_{\text{np}}}\omega t}) - \sqrt{\Delta_{g_{\text{np}}}\omega t}]^2}{\Delta_{g_{\text{np}}}^3} \text{Var}[\hat{X}^2]_{|\phi\rangle_b}, \quad (19)$$

where $\hat{X} = (a + a^\dagger)/\sqrt{2}$ and $|\phi\rangle_b$ is the initial state of the bosonic field. In Fig. 3, the QFI as a function of the evolution time t is shown for different parameters g . It's not difficult to see that $\mathcal{I}_{g_{\text{np}}}$ tends to infinity as $g \rightarrow 1$ (i.e., $\Delta_{\text{np}} \rightarrow 0$), and therefore we can improve the accuracy of evaluating the parameter by critical quantum dynamics.

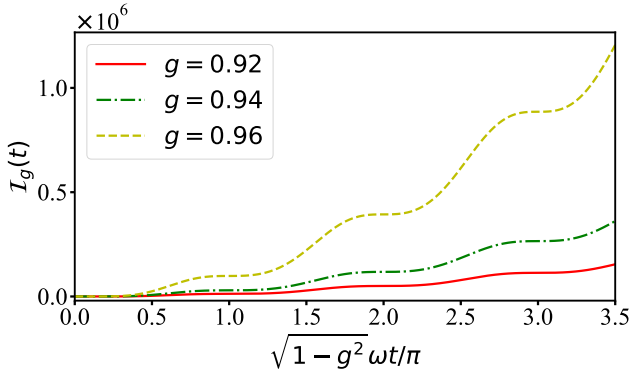


FIG. 3. Sensing with the KRM by homodyne detection of the bosonic field. The QFI $\mathcal{I}_g(t)$ as a function of the evolution time t in the normal phase.

With the same analysis, we can obtain the QFI in the superradiant phase as

$$\mathcal{I}_{g_{\text{sp}}}(t) \approx 256g^2 \frac{[\sin(\sqrt{\Delta_{g_{\text{sp}}}\omega t}) - \sqrt{\Delta_{g_{\text{sp}}}\omega t}]^2}{\Delta_{g_{\text{sp}}}^3} \text{Var}[\hat{X}^2]_{|\phi\rangle_b}, \quad (20)$$

where $\Delta_{g_{\text{sp}}} = 16g(g-1) \ll 1$. Under the condition $\text{Var}[\hat{X}^2]_{|\phi\rangle_b}$ is non-zero, such a scaling of $\mathcal{I}_{g_{\text{sp}}}(t) \propto \Delta_{g_{\text{sp}}}^{-3}$ holds, which is valid for general initial states. From Fig. 4, we can see that the QFI in the superradiant phase also tends to infinity as $g \rightarrow 1$, which is the same as the normal phase.

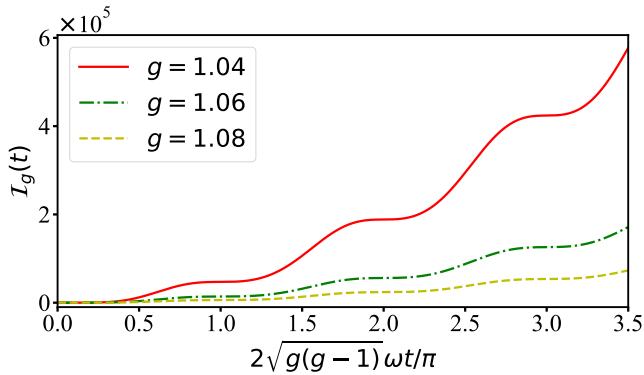


FIG. 4. The QFI $\mathcal{I}_g(t)$ as a function of the evolution time t in the superradiant phase.

IV. CRITICALITY-ENHANCED SUSCEPTIBILITY

In this paper, we consider the quadrature measurements of the bosonic field for standard homodyne detection. Homodyne detection depends on projecting on the quadrature operator $\hat{P} = i(a^\dagger - a)/\sqrt{2}$. With no loss of generality, here we set the initial state of the bosonic field

$|\phi\rangle_b = (|0\rangle + |1\rangle)/\sqrt{2}$. After an evolution time t , we can obtain the mean value and variance of the quadrature operator \hat{P} in the normal phase as

$$\langle P \rangle_t = -\sqrt{2}(1+g)\Delta_g^{-1/2}\sin(\sqrt{\Delta_g}\omega t/2) \quad (21)$$

and

$$(\Delta P)^2 = 1 + \frac{3g-1}{4(1-g)}[1 - \cos(2\omega t\sqrt{1-g^2})], \quad (22)$$

respectively.

The susceptibility of the observable $\langle P \rangle_t$ is a function of the parameter g , i.e., $\chi_g(t) = \partial_g \langle P \rangle_t$ and becomes divergent when g is close to the critical point. To clearly demonstrate the precision of the parameter estimation, we define the inverted variance $\mathcal{F}_g = \chi_g^2/(\Delta P)^2$. When comparing $\mathcal{F}_g(t)$ and $\mathcal{I}_g(t)$, we find that the former is generally smaller than the latter. The precision reaches the ultimate precision of quantum parameter estimation given by the quantum Cramér-Rao if $\mathcal{F}_g(t) = \mathcal{I}_g(t)$. Obviously, the inverted variance reaches its local maximums at the evolution time $\tau_n = 2n\pi/(\sqrt{\Delta_{g_{\text{np}}}\omega}) (n \in \mathbb{Z}^+)$, i.e.,

$$\mathcal{F}_{g_{\text{np}}}(\tau_n) = 32\pi^2 g^2 (1+g)^2 \Delta_{g_{\text{np}}}^{-3} n^2. \quad (23)$$

In addition, we can obtain the QFI $\mathcal{I}_{g_{\text{np}}}(\tau_n) \simeq 64\pi^2(1+g)^2 \Delta_{g_{\text{np}}}^{-3} n^2 \text{Var}[\hat{X}^2]_{|\phi\rangle_b}$ from Eq. (19).

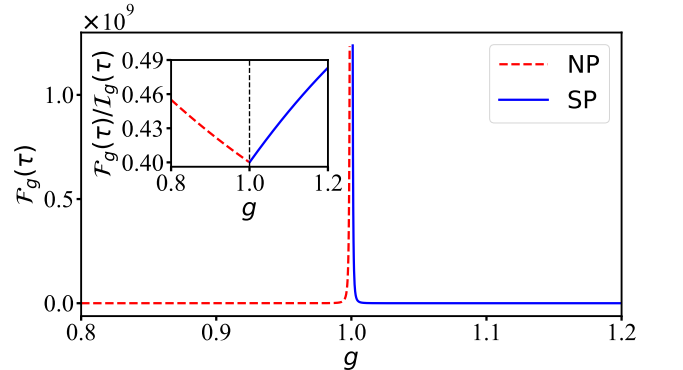


FIG. 5. The inverted variance $\mathcal{F}_g(\tau_n)$ as a function of the parameter g . Inset: for an evolution time $\tau = 2\pi/(\sqrt{\Delta_g}\omega)$, the local maximum of the inverted variance $\mathcal{F}_g(\tau_n)$ arrives at the same order of $\mathcal{I}_g(\tau)$.

We can obtain the inverted variance in the superradiant phase with a similar analysis by which we derive Eq. (23) as

$$\mathcal{F}_{g_{\text{sp}}}(\tau_n) = 512\pi^2 g^2 (2g-1)^2 \Delta_{g_{\text{sp}}}^{-3} n^2, \quad (24)$$

where $\Delta_{g_{\text{sp}}} = 16g(g-1)$.

In Fig. 5, the inverted variance exhibits a divergent behavior at $g = 1$. To a certain extent, we can see that the inverted variance $\mathcal{F}_g(\tau_n)$ and the QFI are on the same order of magnitude from the inset in Fig. 5 and thus we can compare $\mathcal{F}_g(\tau_n)$ with the QFI. It is worth noting

that this result does not depend on any specific initial states of the bosonic field. Besides, we find that as the evolution time τ_n increases, we can obtain larger $\mathcal{F}_g(\tau_n)$ value, indicating a higher precision.

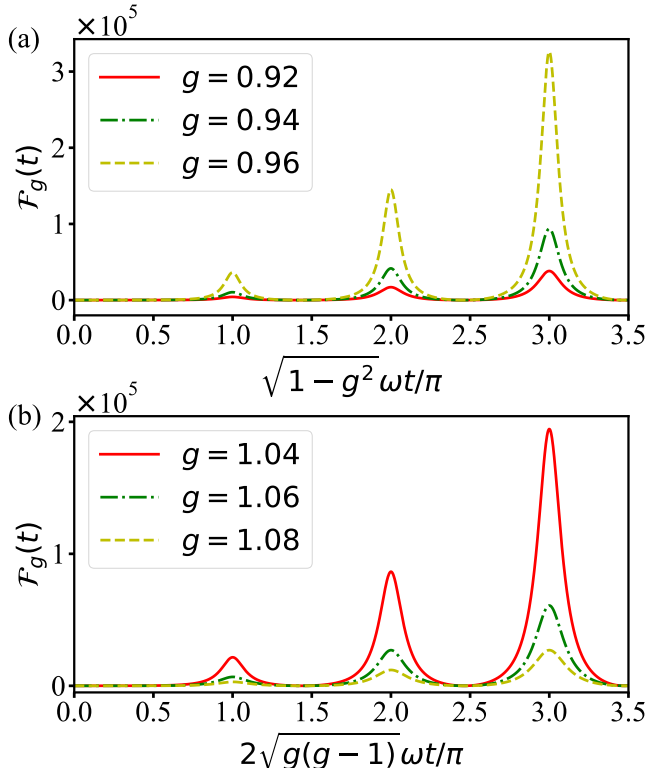


FIG. 6. The inverted variance $\mathcal{F}_g(t)$ as a function of the evolution time t for (a) in the normal phase and for (b) in the superradiant phase.

From Fig. 6, one can easily obtain that the inverted variance achieves its local maximums at $t = 2n\pi/(\sqrt{\Delta_g}\omega)(n \in \mathbb{Z}^+)$ and its peak has a certain width, indicating that the inverted variance can maintain a large value in a great measure in a small range of the evolution time in the normal phase (a) and in the superradiant phase (b).

Next let's discuss the influence of finite χ on the inverted variance $\mathcal{F}_g(\tau)$. It can be seen from Fig. 7 that as the parameter g approaches 1, the value of χ plays an important role in reducing the ratio of $\mathcal{F}_g^\chi(\tau)/\mathcal{F}_g(\tau)$, in-

dicating the lower precision of the parameter estimation. Furthermore, one can easily see that when the order of magnitude of χ is about 10 to the negative 5th power, the precision can maintain a high value.

V. CONCLUSION

In conclusion, we have proposed a scheme for realizing quantum critical metrology with a single parameterically-driven Kerr resonator. In the scheme, the signal is encoded in one of the quadratures of the photonic field

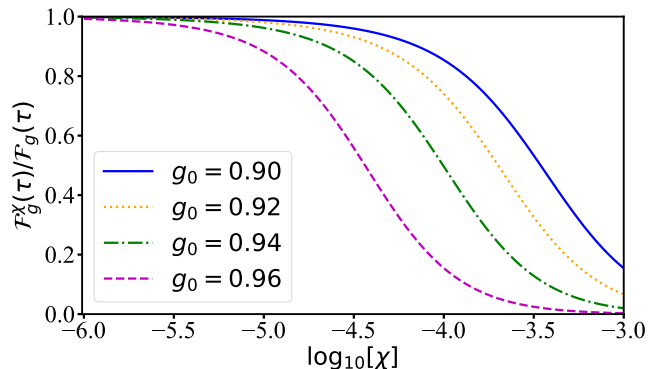


FIG. 7. The ratio between the inverted variance $\mathcal{F}_g^\chi(\tau)$ for finite χ and the ideal value $\mathcal{F}_g(\tau)$ for different values of g after an evolution $\tau = 2\pi/(\sqrt{\Delta_g}\omega)$.

stored in the resonator. We quantify the sensitivity with the quantum Fisher information, which exhibits an oscillatory behavior near the critical point, with the local maximum nonlinearly scaling with the evolution time. The results show that the criticality enhancement is achieved no matter whether the system works below or above the critical point. The critical system can be realized with the presently available techniques in superconducting circuits [16].

ACKNOWLEDGMENTS

This work was supported by the National Natural Science Foundation of China (Grants No. 12274080, No. 11874114, and No. 11875108).

[1] S. Sachdev, *Quantum Phase Transitions* (Cambridge University Press, 2000).
 [2] S. L. Sondhi, S. M. Girvin, J. P. Carini, and D. Shahar, Continuous quantum phase transitions, *Rev. Mod. Phys.* **69**, 315 (1997).
 [3] K. Macieszczak, M. Guță, I. Lesanovsky, and J. P. Garrahan, Dynamical phase transitions as a resource for quantum enhanced metrology, *Phys. Rev. A* **93**, 022103

(2016).
 [4] S. Fernández-Lorenzo and D. Porras, Quantum sensing close to a dissipative phase transition: Symmetry breaking and criticality as metrological resources, *Phys. Rev. A* **96**, 013817 (2017).
 [5] T. Ilias, D. Yang, S. F. Huelga, and M. B. Plenio, Criticality-enhanced quantum sensing via continuous measurement, *PRX Quantum* **3**, 010354 (2022).

- [6] L. Garbe, O. Abah, S. Felicetti, and R. Puebla, Critical quantum metrology with fully-connected models: from Heisenberg to Kibble–Zurek scaling, *Quantum Sci. Technol.* **7**, 035010 (2022).
- [7] L. Garbe, M. Bina, A. Keller, M. G. A. Paris, and S. Felicetti, Critical quantum metrology with a finite-component quantum phase transition, *Phys. Rev. Lett.* **124**, 120504 (2020).
- [8] Y. Chu, S. Zhang, B. Yu, and J. Cai, Dynamic framework for criticality-enhanced quantum sensing, *Phys. Rev. Lett.* **126**, 010502 (2021).
- [9] X. Zhu, J.-H. Lü, W. Ning, F. Wu, L.-T. Shen, Z.-B. Yang, and S.-B. Zheng, Criticality-enhanced quantum sensing in the anisotropic quantum rabi model, *Sci. China Phys. Mech. Astron.* **66**, 250313 (2023).
- [10] J.-H. Lü, W. Ning, X. Zhu, F. Wu, L.-T. Shen, Z.-B. Yang, and S.-B. Zheng, Critical quantum sensing based on the jaynes-cummings model with a squeezing drive, *Phys. Rev. A* **106**, 062616 (2022).
- [11] S. Gammelmark and K. Mølmer, Phase transitions and heisenberg limited metrology in an ising chain interacting with a single-mode cavity field, *New J. Phys.* **13**, 053035 (2011).
- [12] R. Di Candia, F. Minganti, K. V. Petrovnin, G. S. Paraoanu, and S. Felicetti, Critical parametric quantum sensing, *npj Quantum Inf* **9**, 23 (2023).
- [13] E. Grigoriou and C. Navarrete-Benlloch, Signatures of a quantum phase transition on a single-mode bosonic model (2023), [arXiv:2303.12894](https://arxiv.org/abs/2303.12894).
- [14] S. Puri, S. Boutin, and A. Blais, Engineering the quantum states of light in a kerr-nonlinear resonator by two-photon driving, *npj Quantum Inf* **3**, 18 (2017).
- [15] S. Puri, L. St-Jean, J. A. Gross, A. Grimm, N. E. Frattini, P. S. Iyer, A. Krishna, S. Touzard, L. Jiang, A. Blais, S. T. Flammia, and S. M. Girvin, Bias-preserving gates with stabilized cat qubits, *Sci. Adv.* **6**, eaay5901 (2020).
- [16] A. Grimm, N. E. Frattini, S. Puri, S. O. Mundhada, S. Touzard, M. Mirrahimi, S. M. Girvin, S. Shankar, and M. H. Devoret, Stabilization and operation of a kerr-cat qubit, *Nature* **584**, 205 (2020).
- [17] F. Minganti, N. Bartolo, J. Lolli, W. Casteels, and C. Ciuti, Exact results for Schrödinger cats in driven-dissipative systems and their feedback control, *Sci. Rep.* **6**, 26987 (2016).
- [18] N. Bartolo, F. Minganti, W. Casteels, and C. Ciuti, Exact steady state of a kerr resonator with one- and two-photon driving and dissipation: Controllable wigner-function multimodality and dissipative phase transitions, *Phys. Rev. A* **94**, 033841 (2016).
- [19] D. Roberts and A. A. Clerk, Driven-dissipative quantum kerr resonators: New exact solutions, photon blockade and quantum bistability, *Phys. Rev. X* **10**, 021022 (2020).
- [20] M. Raghunandan, J. Wrachtrup, and H. Weimer, High-density quantum sensing with dissipative first order transitions, *Phys. Rev. Lett.* **120**, 150501 (2018).
- [21] F. Reiter, A. S. Sørensen, P. Zoller, and C. A. Muschik, Dissipative quantum error correction and application to quantum sensing with trapped ions, *Nat. Commun.* **8**, 1822 (2017).
- [22] Y. Xie, J. Geng, H. Yu, X. Rong, Y. Wang, and J. Du, Dissipative quantum sensing with a magnetometer based on nitrogen-vacancy centers in diamond, *Phys. Rev. Appl.* **14**, 014013 (2020).
- [23] S. Wald, S. V. Moreira, and F. L. Semião, In- and out-of-equilibrium quantum metrology with mean-field quantum criticality, *Phys. Rev. E* **101**, 052107 (2020).
- [24] T. L. Heugel, M. Biondi, O. Zilberberg, and R. Chitra, Quantum transducer using a parametric driven-dissipative phase transition, *Phys. Rev. Lett.* **123**, 173601 (2019).
- [25] M. Soriente, T. L. Heugel, K. Omiya, R. Chitra, and O. Zilberberg, Distinctive class of dissipation-induced phase transitions and their universal characteristics, *Phys. Rev. Res.* **3**, 023100 (2021).
- [26] C. Chen, P. Wang, and R.-B. Liu, Effects of local decoherence on quantum critical metrology, *Phys. Rev. A* **104**, L020601 (2021).
- [27] S. Pang and A. N. Jordan, Optimal adaptive control for quantum metrology with time-dependent Hamiltonians, *Nat. Commun.* **8**, 14695 (2017).
- [28] S. Pang and T. A. Brun, Quantum metrology for a general hamiltonian parameter, *Phys. Rev. A* **90**, 022117 (2014).